1082-2-Q = RL-2024

Copy

THE UNIVERSITY OF MICHIGAN

COLLEGE OF ENGINEERING

DEPARTMENT OF ELECTRICAL ENGINEERING

Radiation Laboratory

DOPPLER RADIATION STUDY

Quarterly Report No. 2

1 October 1967 - 1 January 1968

By

Chiao-Min Chu, Joseph E. Ferris and Andrew M. Lugg

15 January 1968

Contract No. N62269-67-C-0545

Contract With: The U. S. Naval Air Development Center
Johnsville, Warminster, PA. 18974

Administered through:
OFFICE OF RESEARCH ADMINISTRATION · ANN ARBOR

TABLE OF CONTENTS

ABSTRACT

In this, the Second Quarterly Report on "Doppler Radiation Study", some results of experimental and theoretical investigation are reported.

The measured antenna pattern data for an AN/APN-153 system obtained during the last quarter has been put into digital, three-dimensional format. This digital data will be used in the theoretical calculation of the direct and and reflected radiation.

In the theoretical study, a numerical scheme for calculating the spatial and temporal variations of the reflected radiation, based on a perfectly reflecting ground, is formulated. Schemes for presenting the numerical results in terms of 'normalized coordinates' are also considered. For the minimum detectable signal and gain of the possible receiving system, the approximate signal ranges are calculated.

I INTRODUCTION

This is the Second Quarterly Report on Contract N62269-67-C-0545, "Doppler Radiation Study" and covers the period 1 October 1967 through 1 January 1968.

The primary objective of this project is to characterize the radiation from airborne doppler navigational radar systems, and the probability of detection of such radiation.

During the present research period, the following research has been accomplished.

1. The measured radiation pattern of an AN/APN-153 antenna has been put in digital form. Such a form is useful for the numerical calculations of the spatial and temporal distributions of the radiation transmitted from the antenna.

2. Techniques for the computation of the spatial and temporal distribution of the radiation reflected by a smooth perfectly reflecting ground is formulated. After various considerations and trials, a means of presenting the power level of the reflected radiation in terms of normalized coordinates are introduced. The possibility of approximating the actual radiation pattern by an equivalent Gaussian distribution is also carried out.

3. Techniques for the computation of the radiation reflected from a diffusely reflecting ground is also being started. This phase of the work, however, is not included in this report because of the somewhat more tedious algebraic expressions involved .

During the next research period, the numerical scheme for the calculation of the reflected radiation from a diffusely reflecting ground will be continued. The possibility of approximati ng the actual radiation pattern

by an equivalent Gaussian distribution to simplify the computational scheme will be carried out.

The computational scheme for the reflected radiation from a perfectly reflecting ground will be extended to include some typical cases of trapped radiation and multiple reflections due to overcast.

The antenna pattern measurements for the second system of doppler radar will be carried out when they are made available by NADC.

II EXPERIMENTAL STUDY

During the last quarter the three-dimensional pattern data, collected for the AN/APN-153 doppler antenna, has been digitalized and placed in a three-dimensional format. The pattern data was collected for each of the two input ports and is presented in Figs. 1 and 2. All of the pattern data has been normalized with respect to the pattern maximum so that the numbers are represented in db below the pattern maximum. In addition to the data collected by The University of Michigan, four sets of three-dimensional data are presented in Figs. 3 - 6 for the Ryan doppler antenna, APN-182.

Provisions are now being made to equip the NIKE system, available at The University of Michigan, to make fly-by tests of a doppler system during the latter part of March or early April. This refurbishing requires a thorough system checkout of the tracking and missile tracking radar systems and of the communication equipment that will be required to maintain communications between the radar site and the airborne crew.

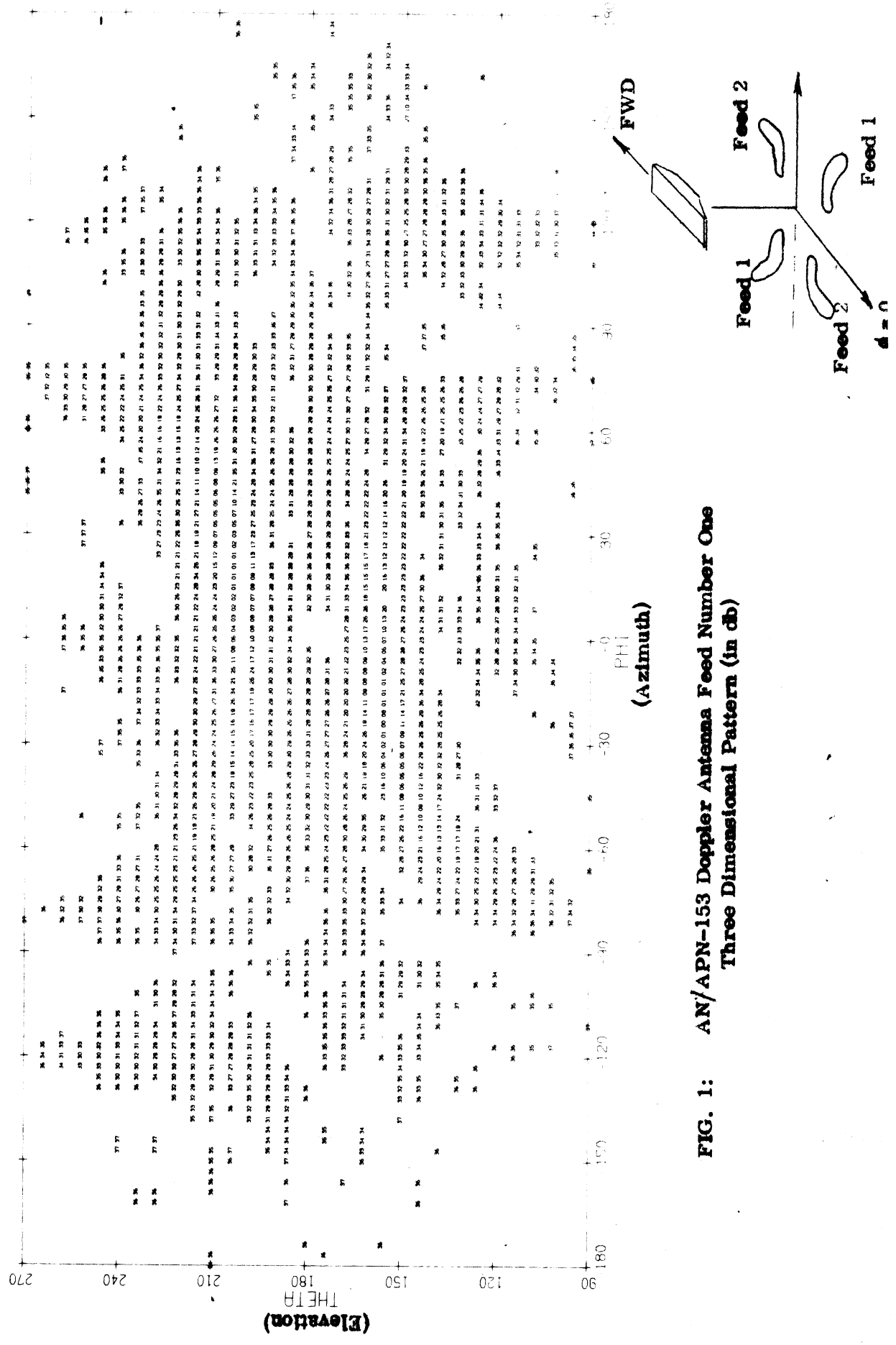

FIG. 1: AN/APN-153 Doppler Antenna Feed Number One Three Dimensional Pattern (in db)

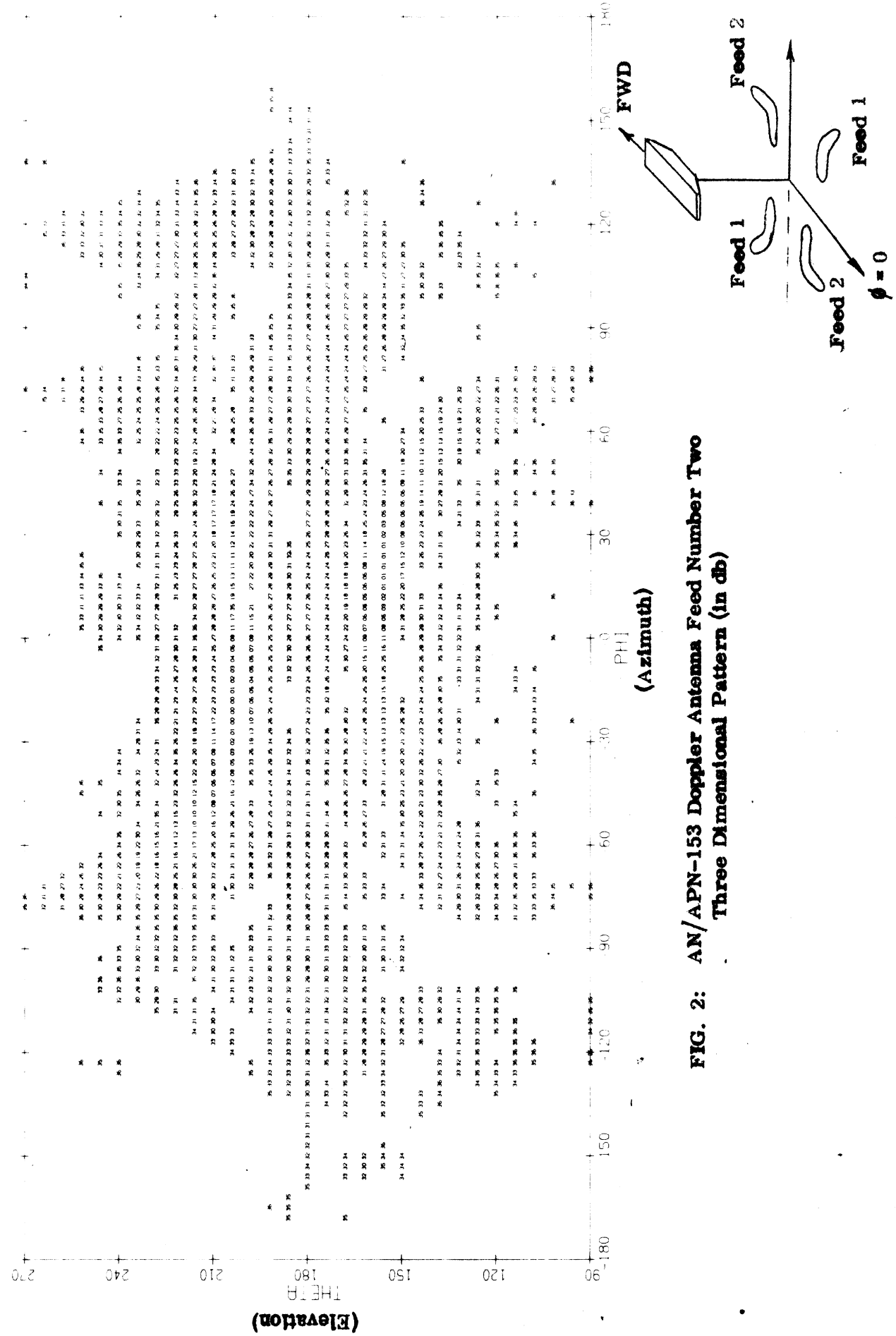

FIG. 2: AN/APN-153 Doppler Antenna Feed Number Two Three Dimensional Pattern (in db)

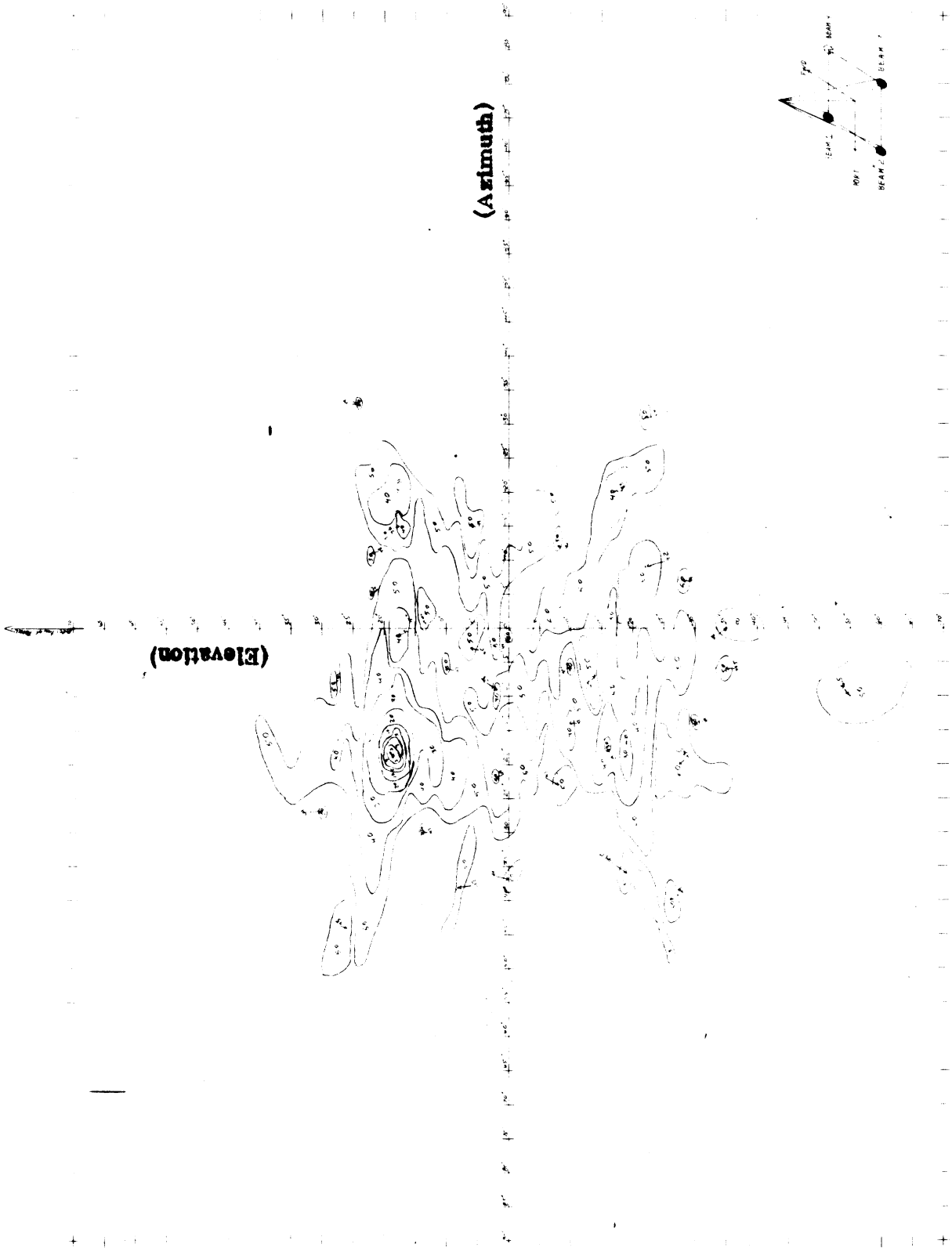

FIG. 3: APN-182 Doppler Antenna Beam Number One (Courtesy Ryan Company)
Three Dimensional Pattern (in db)

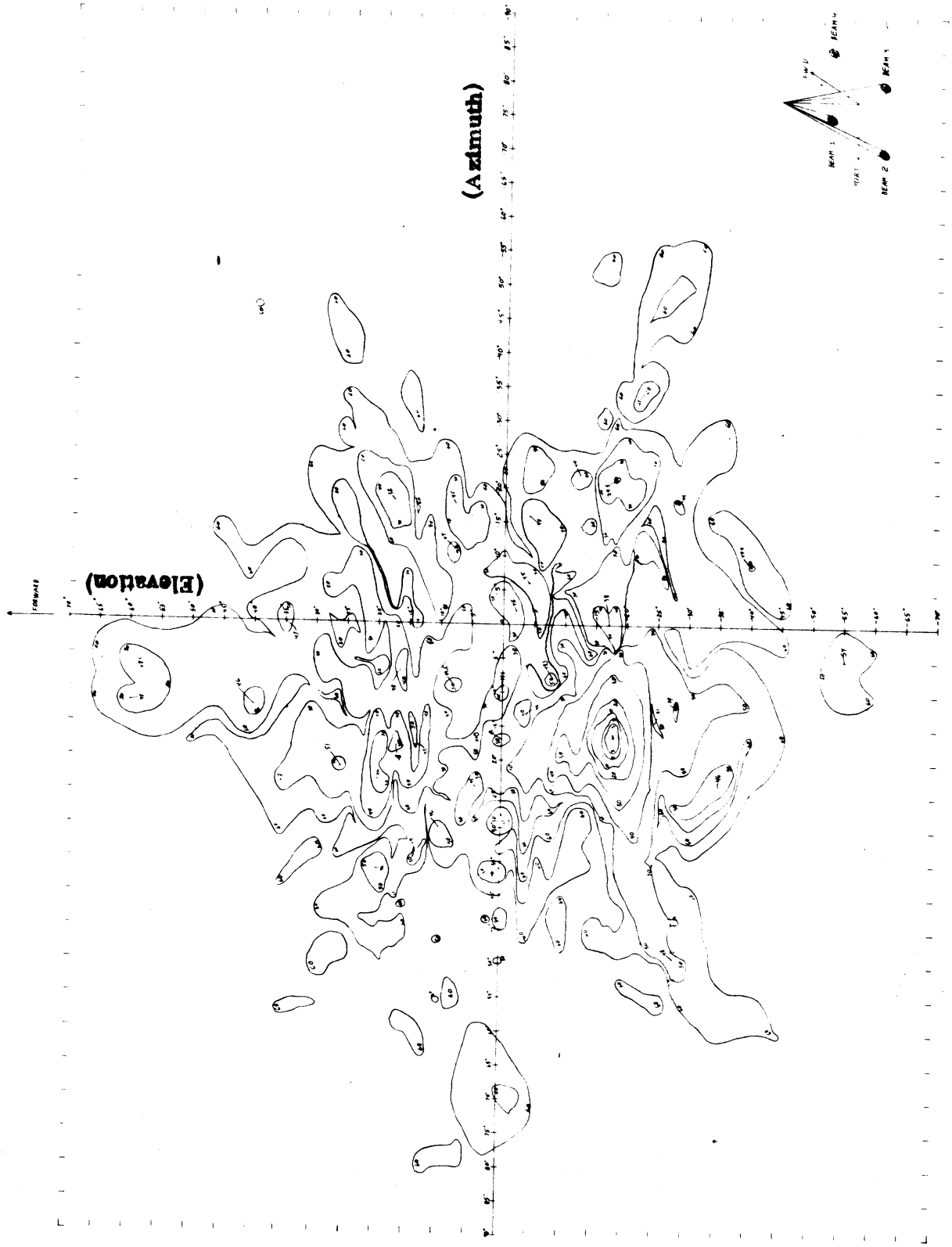

FIG. 4: APN-182 Doppler Antenna Beam Number Two (Courtesy Ryan Company)
Three Dimensional Pattern (in db)

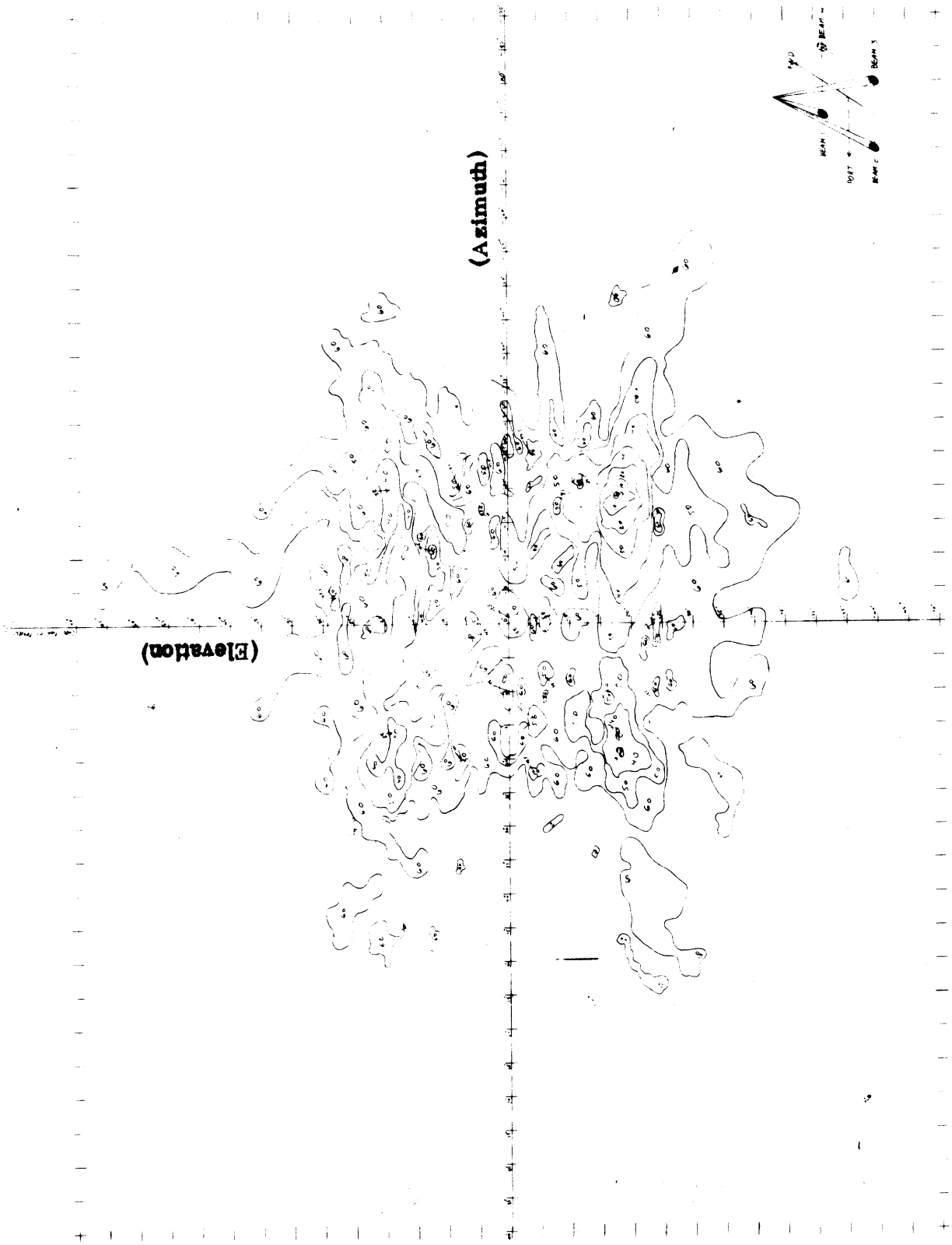

FIG. 5: APN-182 Doppler Antenna Beam Number Three (Courtesy Ryan Company)
Three Dimensional Pattern (in db)

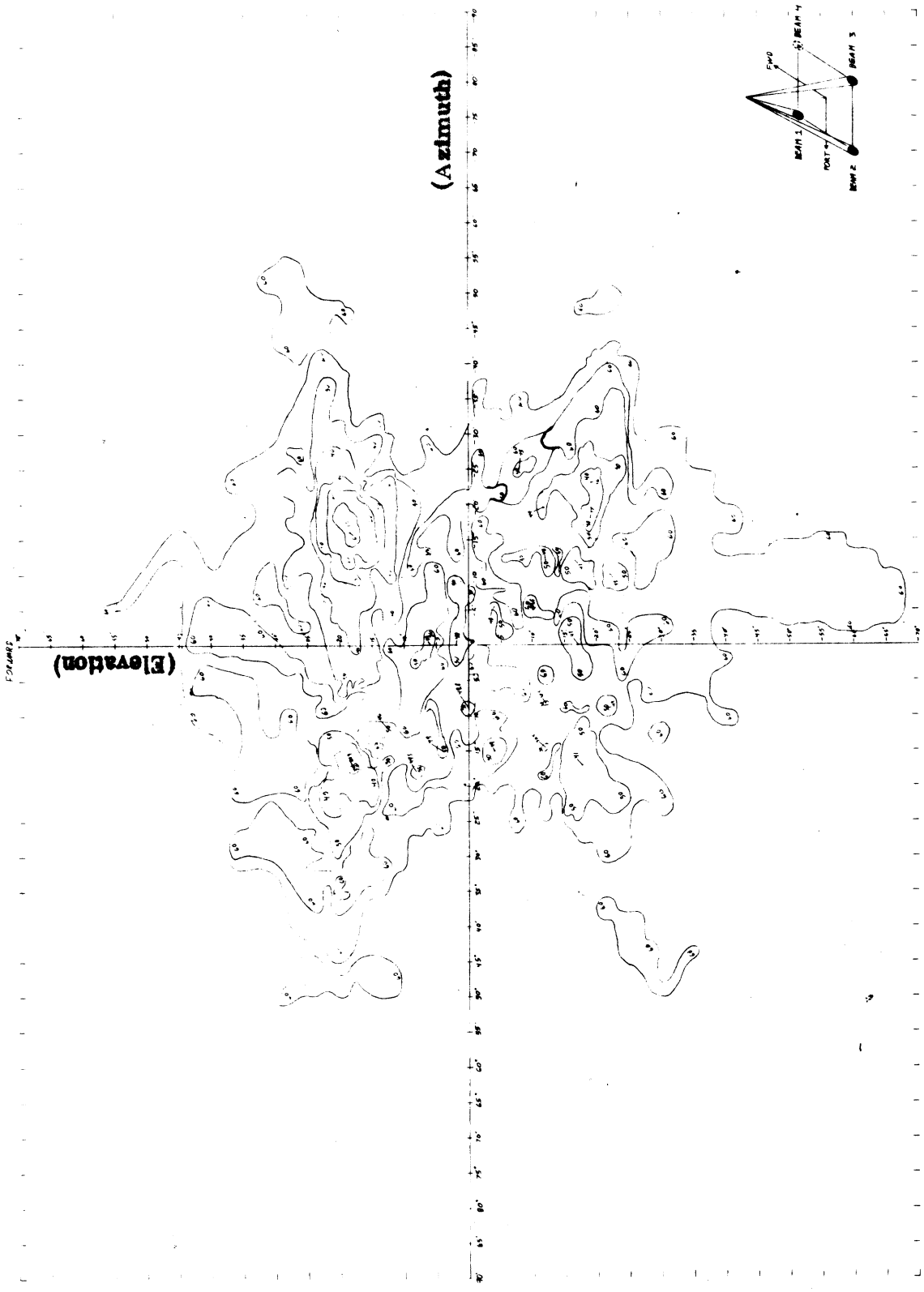

FIG. 6: APN-182 Doppler Antenna Beam Number Four (Courtesy Ryan Company)
Three Dimensional Pattern (in db)

III THEORETICAL STUDY

The numerical scheme of calculating the spatial and temporal distribution of the ground reflected radiation from a doppler radar, and the method of clearly presenting the numerical results, are investigated. Based on geometrical optics, and the digital data of the radiation pattern, the scheme calculation of the spatial and temporal variations of the ground reflected radiation is formulated. The choice of the geometric optics approach is based on the anticipation that this scheme is amenable to extension to trapped and multiply reflecting cases. The scheme for the same calculations in the case of a diffusely reflecting ground is also being investigated but is not completed. This phase of the work is therefore not reported here.

Anticipating that future development in the antennas of doppler systems may be using more narrow beams, approximate calculations for the ground reflected radiation assuming a Gaussian distributed beam is also being carried out and the results are given in Appendices A and B.

3. 1 Spatial Distribution of Specularly Reflected Radiation

From the radiation pattern of the transmitting antenna, the spatial distribution of the transmitted radiation reflected specularly from the ground may be calculated by the method of Images. Figure 7 shows that the radiation from a transmitter at a position (x_a, y_a, z_a) in the direction (θ, ϕ) would, after reflection from the ground, reach a height h at the point (x_h, y_h, h). A simple geometric argument yields

$$\begin{aligned} x_h &= -(z_a+h)\tan\theta\cos\phi+x_a \\ y_h &= -(z_a+h)\tan\theta\sin\phi+y_a \end{aligned} \qquad (3.1)$$

The distance travelled by the reflected radiation is then

$$R(h, \theta, \phi) = \sqrt{(z_a+h)^2+(x_h-x_a)^2+(y_h-y_a)^2} \qquad (3.2)$$

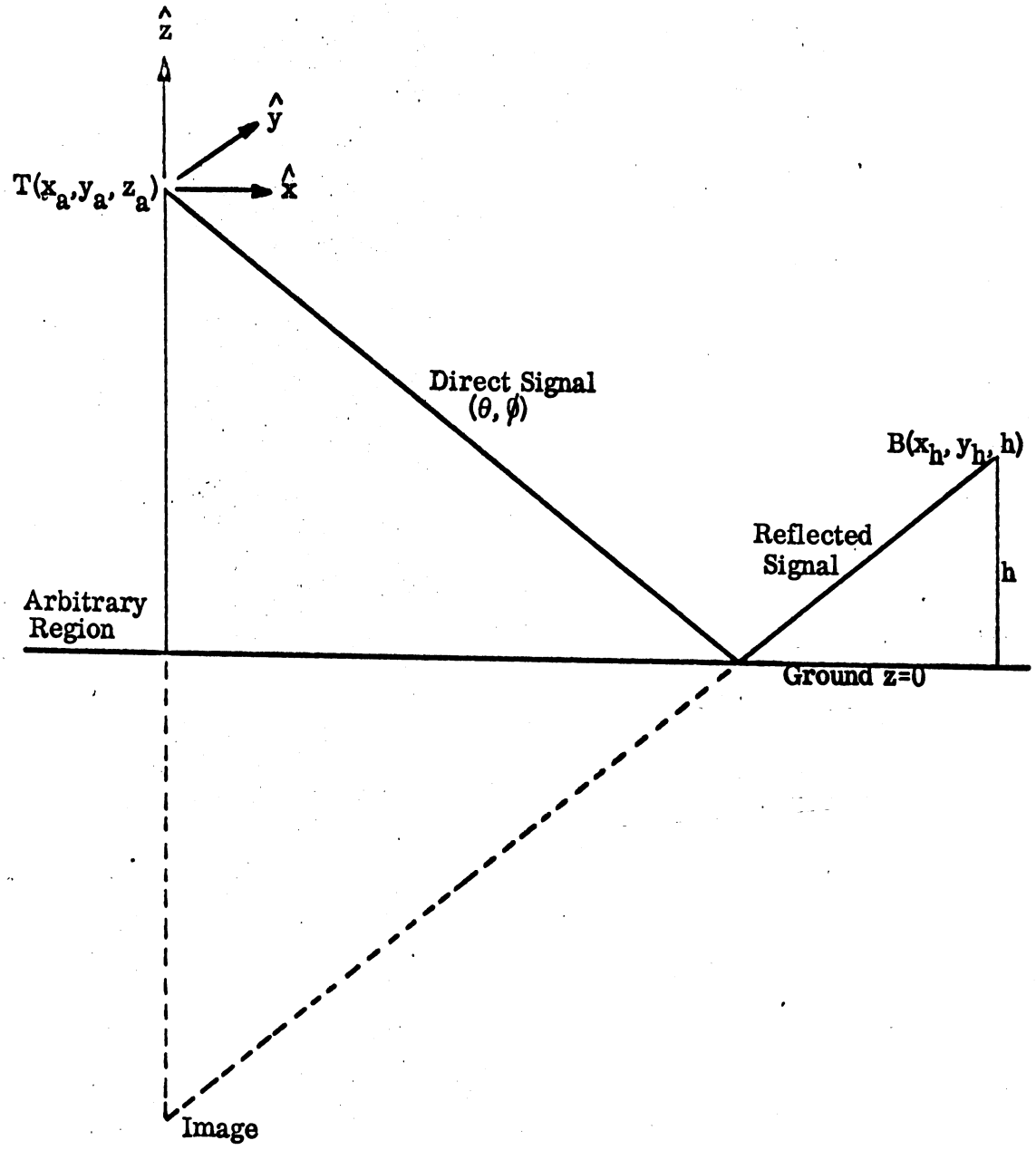

FIG. 7: GEOMETRY FOR REFLECTED RAY

Thus, the power radiated from the transmitter T would, after reflection, reach the point B after a time delay of

$$\tau\,(h, \theta, \phi) = \frac{R(h, \theta, \phi)}{c} \tag{3.3}$$

where c is the velocity of light.

Moreover, the power received from the ground reflection is different at different points of observation. To investigate the spatial variation of the reflected signal, it is therefore more convenient to investigate the variation of the reflected power observed at points in a horizontal plane of fixed h (i. e. for fixed height of receiver). For the convenience of numerical calculation and display of results, the following normalized coordinates are defined.

a) The relative height

$$\xi \triangleq \frac{z_a - h}{z_a + h} \tag{3.4}$$

b) The relative horizontal coordinates

$$X = X(\theta, \phi, \xi) \triangleq \frac{x_h - x_a}{z_a} = -\frac{2}{1+\xi} \tan\theta \cos\phi \tag{3.5}$$

$$Y = Y(\theta, \phi, \xi) \triangleq \frac{x_h - x_a}{z_a} = -\frac{2}{1+\xi} \tan\theta \sin\phi \tag{3.6}$$

Using these relations, one finds that

$$R = z_a \sqrt{X^2 + Y^2 + \left(\frac{2}{1+\xi}\right)^2}\,. \tag{3.7}$$

For the variation of radiated power across a horizontal plane we use Eq. (3.18) of the First Quarterly Report[+], which states that the amplitude of electric field is

---

[+] Chu, C-M, J. E. Ferris and A. M. Lugg (1967), "Doppler Radiation Study," The University of Michigan Report 1082-1-Q.

$$E(x_h, y_h) = \frac{p}{-(z_a+h)\tan\theta} \quad f(\theta, \phi) \tag{3.8}$$

where p is related to the gain of the antenna, G_t, and the total power radiated, P. From the radiation pattern in the digitized form, we find that there is a direction (θ_M, ϕ_M) at which $f(\theta_M, \phi_M) = 1$, corresponding to 0 db in the chart. It is evidently more convenient to refer to the received power level (in db down) to this direction. Thus, we may denote the power level corresponding to a ray in the direction of θ_M, ϕ_M, i.e., in the direction of the main lobe, at 0 db. At a height h, this ray intersects the point:

$$X_m = -\frac{2}{1+\xi} \tan\theta_m \cos\phi_m \tag{3.9}$$

$$Y_m = -\frac{2}{1+\xi} \tan\theta_m \sin\phi_m \tag{3.10}$$

The ratio of the power level corresponding to a ray in any direction (θ, ϕ) to that corresponding to a ray in the direction of maximum power is,

$$\frac{f^2(\theta, \phi)}{\tan^2\theta} \tan^2\theta_m \tag{3.11}$$

Expressed in decibels, it is therefore:

$$10 \log f^2(\theta, \phi) + 20 \log(\tan\theta_m) - 20 \log(\tan\theta).$$

The term $10 \log f^2(\theta, \phi)$ describes the radiation pattern and its value is obtained from geometrical considerations (cf Appendix A) or from the digitized output of the experimental study. We define this term as follows:

$$db_0(\theta, \phi) \triangleq 10 \log f^2(\theta, \phi). \tag{3.12}$$

To express the power level of reflected rays originating from the transmitter in any direction

$$db_r(\theta,\phi)=db_o(\theta,\phi)+20\log\tan\theta_m-20\log\tan\theta \quad . \tag{3.13}$$

Equation (3.13) together with (3.5) and (3.6) can be used in computing and displaying the relative power level of the specularly reflected radiation from the ground.

The variation of the reflected power level can be cast in a slightly different form to obtain the power level of the direct field strength. This latter power level is usually appreciable when $h < z_a$. For a direct radiated signal in the direction (θ,ϕ) to reach a height h, the normalized coordinates are easily shown to be

$$X^{(d)}(\theta,\phi,\xi) = -\frac{(z_a-h)}{z_n}\tan\theta\cos\phi = -\frac{2\xi}{1+\xi}\tan\theta\cos\phi$$

$$Y^{(d)}(\theta,\phi,\xi) = -\frac{2\xi}{1+\xi}\tan\theta\sin\phi \quad .$$

Thus

$$X^d(\theta,\phi,\xi) = \xi\, X(\theta,\phi,\xi) \qquad \text{and} \qquad Y^d(\theta,\phi,\xi) = \xi\, Y(\theta,\phi,\xi) \; .$$

Furthermore the ratio of field strength of the direct ray to that of the reflected ray is given by

$$\frac{\text{field strength of direct ray}}{\text{field strength of reflected ray}} = \frac{z_a+h}{z_a-h} = \frac{1}{\xi}$$

or, in decibels,

$$(db)_d = (db)_r - 20\log\xi \; . \tag{3.14}$$

Thus, for a fixed $\xi > 0$, the variation in the relative power levels with x and y can be used for both the direct radiation and ground radiation by a change in the X and Y scales. This justifies the use of the parameter ξ in the evaluation and graphical representation of the relative power level.

3.2 Temporal Variations of Reflected Radiation

The analysis given in the previous section for the power level does not take into account possible time variations. In other words, if a short pulse is transmitted from the antenna at a certain time, the power levels are observed at a point in phase, after a time delay given by Eq. (3.1). This time delay, together with the actual motion of the vehicle carrying the radar, determines the temporal variation of the radiation. To bring out some essential features of the temporal variation, let us assume that the vehicle is moving with a horizontal velocity. The trajectory of the moving transmitter is given by $x_a(t)$ and $y_a(t)$. For a receiver at height h and X_o, Y_o at $t_o = 0$, at any time $t > 0$,

$$X(t_o) = \frac{x_a(t_o) - x_h}{z_a} = X_o + \frac{x_a(t_o) - x_a(0)}{z_a}$$

and

$$Y(t_o) = Y_o + \frac{y_a(t_o) - y_a(0)}{z_a}$$

Thus, for a horizontally moving vehicle, the relative power level of the reflected signal at any fixed point may be easily obtained from the power level in the x-y display constructed in Section 3.1 . To illustrate this, let us refer to Fig. 8. For a point defined by (X_o, Y_o) at $t_o = 0$, the trajectory of the moving transmitter may be represented by the locus as indicated . From this curve, we may obtain the variation of the reflected power level as a function of t_o. Let us denote this by

$$db_r(t_o) .$$

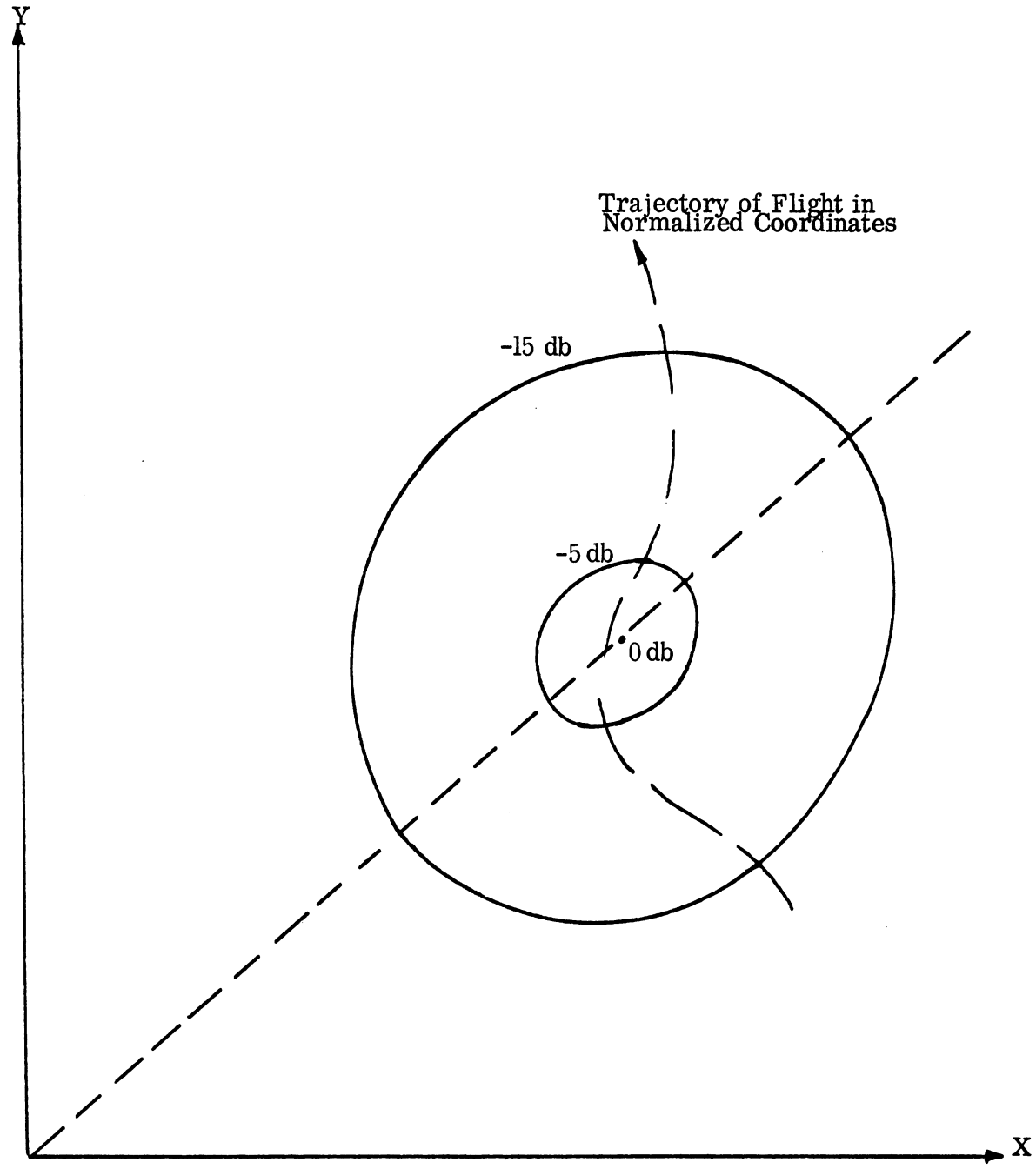

FIG. 8: DIAGRAM SHOWING FLIGHT TRAJECTORY FOR FIXED ξ .

This function, however, is not the relative power level of the received signal because;

a) The transmitted power may be varying. This variation may be represented in db by $db_t(to)$,

b) There is a time delay due to finite velocity of propagation of electromagnetic waves. The position of the signal from the transmitter at t_o, is received at the point of observation at a time

$$t = t_o + \frac{z_a\sqrt{X(t_o)^2+Y(t_o)^2+(\frac{2}{1-\xi})^2}}{c} \quad . \tag{3.15}$$

From the above observations, it is seen that the power level of the received signal as a function of t_o is given by

$$\text{relative power level of receiver system} = db_r(t_o)+db_t(t_o) \quad .$$

This variation, of course, can be transformed into a function of t by using Eq. (3.15).

For an arbitrary direction of flight, i.e., in the ascending or descending phase of flight, x_a, y_a, z_a may all change. Hence for each t_o, $X(t_o), Y(t_o), \xi(t_o)$, should be evaluated for each observation point. The relative power level of the ground reflected radiation as a function of time can then be computed.

At present, a computer program for calculating the relative power level of the reflected radiation is being formulated. However, before attempting any actual calculation, we are investigating possible approximations, and the ranges of parameters for the actual antenna to be used in the doppler system.

3.3 Range and Power Level

It is well known that for a transmitting antenna of output P_t, gain G_t and radiation field pattern $f(\theta, \phi)$, the Poynting vector at a distance R from the

transmitter is

$$\text{Poynting vector} = \frac{P_t}{4\pi R^2} G_t f^2(\theta, \phi) \tag{3.16}$$

For specularly reflected radiation from the ground, this formula also holds provided R is the actual distance traversed by the radiation, such as given by (3.2).

For a receiver at distance R, if the gain of the receiving antenna is G_r, and the frequency of radiation is λ, then the power received is

$$P_r = \frac{P_t G_t f^2(\theta, \phi)}{4\pi R^2} \cdot \frac{\lambda^2 G_r}{4\pi} \tag{3.17}$$

The detectability of the radiation depends on the noise level, the scheme of detection, etc. At present these quantities are not easily specified. However, in general, we may assert that there is a minimum power level above which the signal may be detected. If this minimum detectable signal is denoted by P_N, then the significant range at which the radiation may be detected is given by

$$R = \frac{\lambda}{4\pi} \sqrt{P_t G_t} \sqrt{\frac{G_r}{P_N}} .$$

For the antenna AN/APN-153, which is currently being studied;

$P_t \cong 5$ watts
$G_t \cong 19.5$ db
$f = 13.320$ GHz.

The values of G_r and P_N for a fixed range are plotted in Fig. 9. For the typical values such as $G_r = 20$ db above isotropic, and $P_r = -100$ dbm, it is seen that the reflected signal from the maximum direction, corresponding to the main lobe is detectable at ranges included in the shaded area.

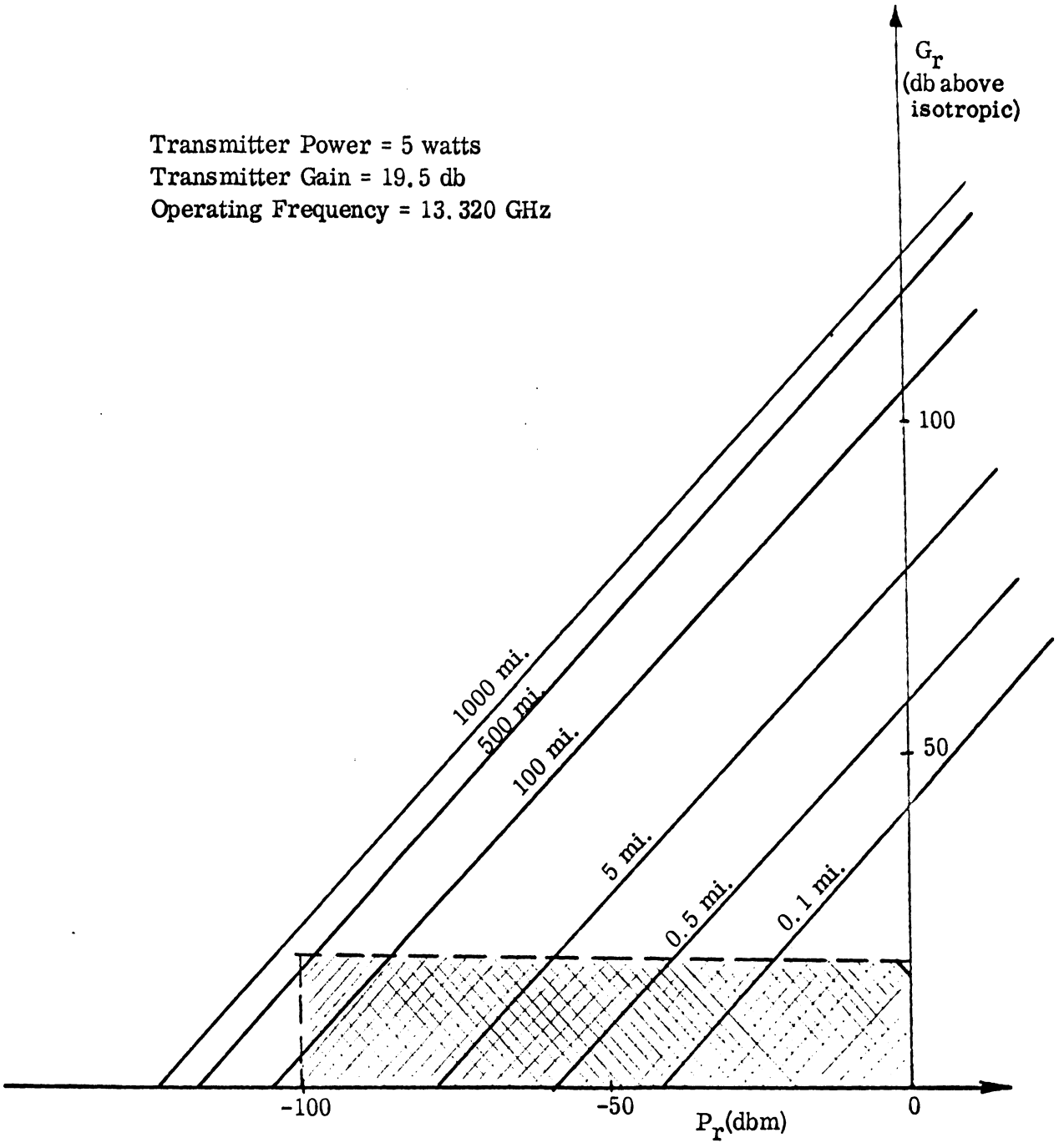

FIG. 9: RECEIVER GAIN VS MINIMUM DETECTABLE SIGNAL POWER FOR VALUES OF SLANT RANGE. (Shaded area indicates region in which aircraft is detectable.)

Now the range indicated in Fig. 9 is the slant range. For any other direction, of course, the range will be smaller. To find the horizontal range the slant range is multiplied by $|\cos\theta|$. From Eq. (3.17) in a direction (θ, ϕ), the horizontal range is:

$$R_H = \frac{\lambda}{4\pi}\sqrt{P_t G_t}\sqrt{\frac{G_r}{P_N}}\, f(\theta,\phi)\,|\sin\theta| \quad .$$

This corresponds to the region,

$$|X| < \frac{\lambda}{4\pi}\sqrt{P_t G_t}\sqrt{\frac{G_r}{P_N}}\,\sin\theta\,|\cos\phi|\, f(\theta,\phi)$$

$$|Y| < \frac{\lambda}{4\pi}\sqrt{P_t G_t}\sqrt{\frac{G_r}{P_N}}\,\sin\theta\,|\sin\phi|\, f(\theta,\phi) \quad .$$

3.4 Approximate Radiation Patterns

For a narrow beam antenna , it is common practice to approximate the actual radiation pattern in terms of a Gaussian distribution

$$f^2(\theta,\phi = \exp\left[-a\,\alpha^2 - b\,\beta^2\right] \qquad (3.18)$$

where α, β are the angular deviation from the direction of maximum radiation along two mutually perpendicular directions normal to the maximum direction. In Appendices A and B, the calculations of spatial and temporal distribution of radiation from an antenna with an approximate radiation pattern is carried out.

To derive the approximations from the actual measured radiation pattern, relations between α, β and θ and ϕ are necessary. In Appendix A, it is shown that if the direction of the maximum radiation is given by (θ_M, ϕ_M), then,

$$\tan(\theta_M + \Delta\theta)\cos(\phi_M + \Delta\phi = \tan(\theta_M + \alpha)\cos\phi_m - \sec\theta_M \tan\beta\,\sin\phi_M \qquad (3.19)$$

$$\tan(\theta_M + \Delta\theta)\sin(\phi_M + \Delta\phi) = \tan(\theta_M + \alpha)\sin\phi_M + \sec\theta_M \tan\beta \cos\phi_M \qquad (3.20)$$

where α and β are angular deviations in the direction of increasing θ and ϕ respectively. In the neighborhood of the maximum direction, we assume that α, β, $\Delta\theta$ and $\Delta\phi$ are small. Then, approximately, by using appropriate small angle approximations of trigonometric functions, it can be shown that

$$\Delta\theta \simeq \alpha \qquad (3.21)$$

$$\Delta\phi \simeq \frac{\sin\theta_M}{\cos^2\theta_M}\,\beta \qquad (3.22)$$

Now, at $\theta = \theta_M$, $\theta = \phi_M$, we know that

$$f^2(\theta, \phi) = 1$$

and

$$\frac{\partial f^2(\theta, \phi}{\partial\theta} = \frac{\partial f^2(\theta, \phi}{\partial\phi} = 0 \quad .$$

Therefore, for most radiation patterns we may approximate

$$f^2(\theta, \phi) \cong 1 - S_1 \Delta\theta^2 - S_2 \Delta\phi^2$$

where

$$S_1 = \frac{\partial^2\left[f^2(\theta, \phi)\right]}{2\,\partial^2\theta} \quad , \qquad S_2 = \frac{\partial^2\left[f^2(\theta, \phi)\right]}{2\,\partial^2\phi}$$

evaluated at θ_M, ϕ_M. Comparing this approximation with the Gaussian distribution for small α and β, which is given by

$$f^2(\theta, \phi) \cong 1 - a\,\alpha^2 - b\,\beta^2$$

we see that a and b are related to the differential quotients S_1 and S_2 by

$$a = \frac{S_1 \Delta\theta^2}{\alpha^2} = S_1 \tag{3.23}$$

and

$$b = \frac{S_2 \Delta\phi^2}{\beta^2} = S_2 \frac{\sin^2 \theta_M}{\cos^4 \theta_M} \tag{3.24}$$

For narrow beam antennas, the approximate distribution given by (3.16), together with the values of a and b determined from the actual radiation pattern is reasonable provided sidelobes do not exist. For patterns with sidelobes we may approximate the pattern by the sum of several terms:

$$f^2(\theta, \phi) = \exp\left[-a\alpha^2 - b\beta^2\right] + A_1 \exp\left[-a_1\alpha_1^2 - b_1\beta_1^2\right] + \ldots\ldots,$$

where A_1 is the value of $f^2(\theta, \phi)$ at the peak of a minor lobe, and a_1, b_1 are determined from (3.23) and (3.24) by using corresponding values of θ, ϕ, S at the minor lobe peak.

APPENDIX A

SPATIAL VARIATIONS IN FIELD STRENGTH FOR A GAUSSIAN BEAM

In general, a normalized electric field strength may be defined. For CW transmitted signal, a suitable normalization is as follows

$$\left|F_h(X,Y)\right| = \left| \frac{E_h\left(X(\theta,\phi), Y(\theta,\phi)\right)}{E_h\left(X(\theta_M,\phi_M), Y(\theta_M,\phi_M)\right)} \right| .$$

From the discussion in Section 3.1, we find

$$\left|F_h(X,Y)\right| = \frac{\sec\theta_M}{\sec\theta} f(\theta,\phi) \quad . \tag{A.1}$$

As suggested in Section 3.4, it is convenient to define another coordinate system. Figure 10 shows the system that we have in mind. The transmitter is situated at T, B_0 is the intersection point of the beam center and a horizontal plane, and the point B is fixed and arbitrary. This observation point, B, is described in terms of the angles θ and ϕ, the depression angle and the azimuthal angle respectively. Thus, the coordinates of B are

$$\left\{+x_a-(z_A+h)\tan\theta\cos\phi\right\}, \left\{y_A-(z_A+h)\tan\theta\sin\phi\right\}, \quad -h \tag{A.2}$$

Alternatively B can be described by utilizing the angles α, β, where α is measured in the 0AB plane about AB and β is measured about AB in a plane perpendicular to 0AB . This coordinate system is introduced to facilitate the computation. It will be seen later that the radiation pattern is expressed more simply when α and β are used than when θ and ϕ are used.

In this system, the coordinates of B are

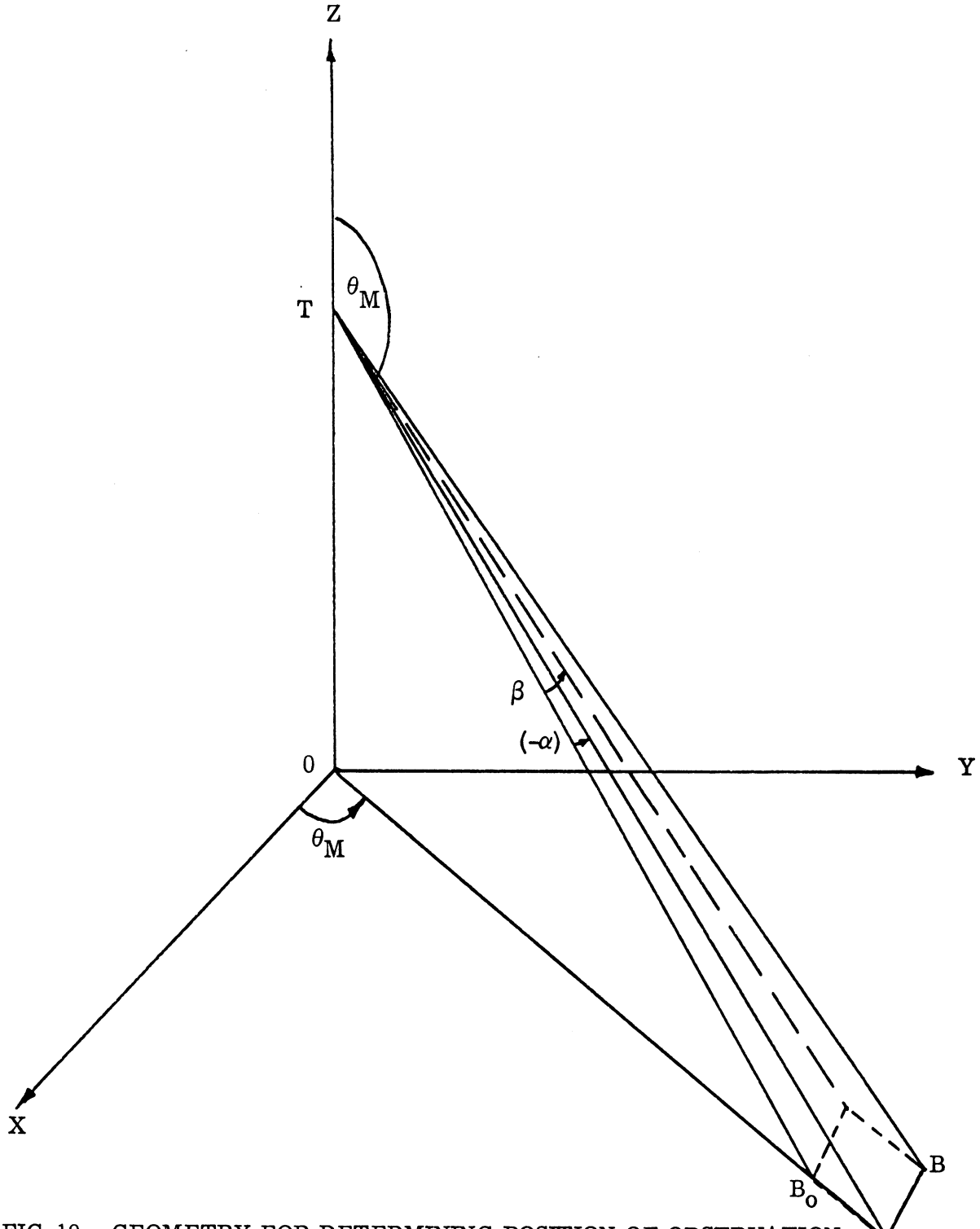

FIG. 10: GEOMETRY FOR DETERMINING POSITION OF OBSERVATION POINT IN TERMS OF ANGLES α, β.

$$\left\{x_A-(z_A+h)\left[\tan(\theta_M+\alpha)\cos\phi_A-\sec\theta_M\tan\beta\sin\phi_A\right]\right\};$$

$$\left\{y_A-(z_A+h)\left[\tan(\theta_M+\alpha)\sin\phi_A+\sec\theta_M\tan\beta\cos\phi_A\right]\right\};$$

$$-h \quad , \tag{A. 3}$$

α and β can be expressed in terms of θ and ϕ by equating distances in expressions (A. 2) and (A. 3) and recalling that $\theta \triangleq \theta_M+\Delta\theta$ and $\phi \triangleq \theta_M+\Delta\phi$. The results are given by Eqs. (3. 17) and (3. 18). Alternatively we may write:

$$\begin{bmatrix}\tan(\theta_M+\alpha)\\ \sec\theta_M\tan\beta\end{bmatrix} = \tan(\theta_M+\Delta\theta)\begin{bmatrix}\cos\phi & \sin\phi\\ \sin\phi & -\cos\phi\end{bmatrix}\begin{bmatrix}\cos\phi_A\\ \sin\phi_A\end{bmatrix} \tag{A. 4}$$

Using this transformation (A. 1) may be written as

$$\left|F_h(X, Y)\right| = \frac{\sec\theta_M\, f(\alpha,\ \beta)}{\left\{\sec^2(\theta_M+\alpha)+\sec^2\theta_M\tan^2\beta\right\}^{1/2}}$$

where for a Gaussian beam

$$f(\alpha, \beta) \triangleq \exp\left[-\frac{1}{2}(a_1^2\alpha^2+b_1^2\beta^2\right]$$

and for a beam with sidelobes

$$f(\alpha, \beta) \triangleq 64\,\frac{J_2(a_2\alpha)}{(a_2\alpha)^2}\quad\frac{J_2(b_2\beta)}{(b_2\beta)^2}$$

where a_1, b_1 etc may be calculated from Eqs. (3. 21) and (3. 22) or from the following expressions:

$$a_1 = \frac{1.388}{\Theta_{a_1}} \quad ; \qquad b_1 = \frac{1.388}{\Theta_{b_1}} \quad ; \quad a_2 = \frac{1.27\pi}{\Theta_{a_2}} \quad ; \quad b_2 = \frac{1.27\pi}{\Theta_{b_2}}$$

and Θ_{a_1}, Θ_{a_2}, etc are the respective beamwidths.

Figure 11 shows the pattern functions for beamwidths of 8° and Fig. 12 shows a plot of the power distribution of these functions.

Consider a Gaussian distributed beam; then

$$\left|F_h(X, Y)\right| = \frac{\sec\theta_M \, e^{-\frac{1}{2}(a^2\alpha^2+b^2\beta^2)}}{\left\{\sec^2(\theta_M-\alpha)+\sec^2\theta_M\tan^2\beta\right\}^{1/2}} \qquad (A.5)$$

where the position X, Y is given indirectly by (A.3). For small α, β the variation in the exponential term dominates the expression. As α, β increase the magnitude of $F_h(X, Y)$ decreases rapidly. Because we are particularly interested in the region in which the signal power is discernible by some monitoring device, we can write as a first approximation

$$\left|F_h(X, Y)\right| \simeq \exp\left[-\frac{1}{2}(a^2\alpha^2+b^2\beta^2)\right] \qquad (A.6)$$

If the reflected radiation at some α, β is Δdb down on the power at $\alpha = \beta = 0$, the following relation results

$$a^2\alpha^2+b^2\beta^2 = \frac{\Delta \log_e 10}{10} \qquad (A.7)$$

Equation (A. 7) defines contours of electric field strength in the X, Y plane for a fixed height, h. By way of example, we choose $a = b = 0.277/^{\circ}$, i.e. a 5° beamwidth in both the α and β directions. The contours are given by $\alpha^2+\beta^2 = 3\Delta$.

Figure 13 shows such electric field strength variations in the X, Y plane. Furthermore a similar expression for the direct radiation can be found as described in the body of this report (see Eq. (3. 14)). The direct radiation pattern is shown in Fig. 14 for $\xi = 1/2$.

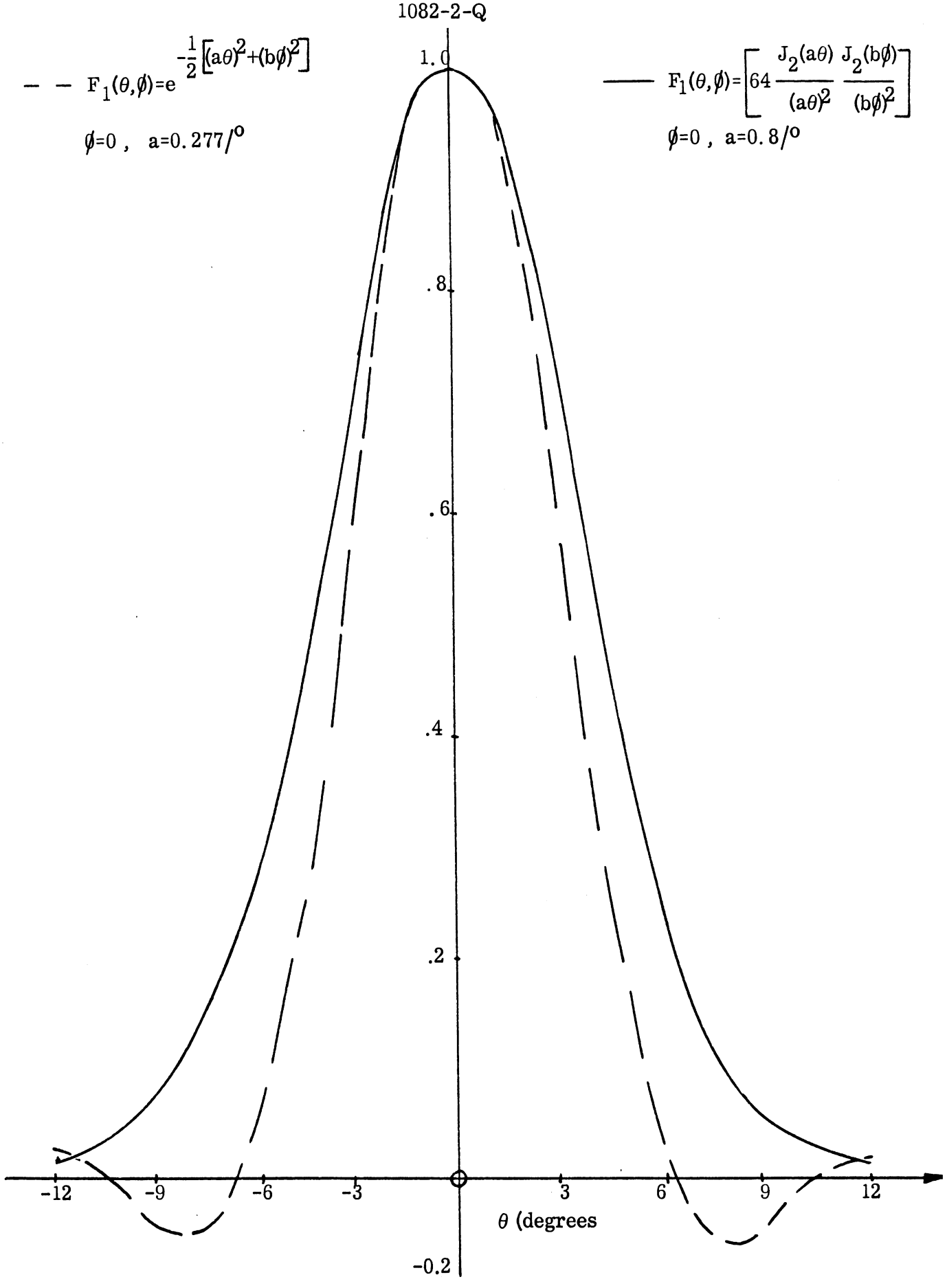

FIG. 11: PATTERN FUNCTION FOR BEAMWIDTH = 5°.

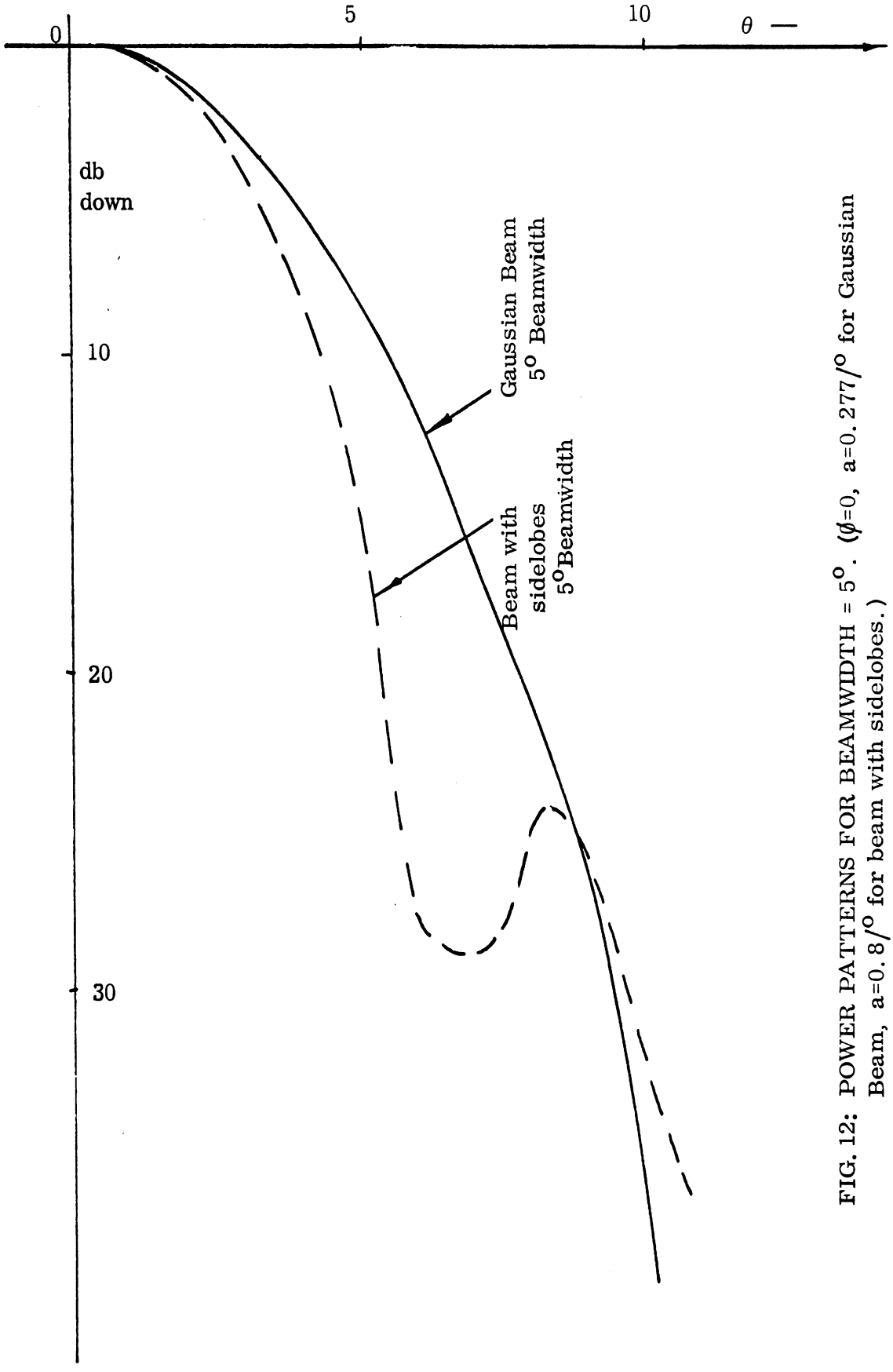

FIG. 12: POWER PATTERNS FOR BEAMWIDTH = 5°. (ϕ=0, a=0.277/° for Gaussian Beam, a=0.8/° for beam with sidelobes.)

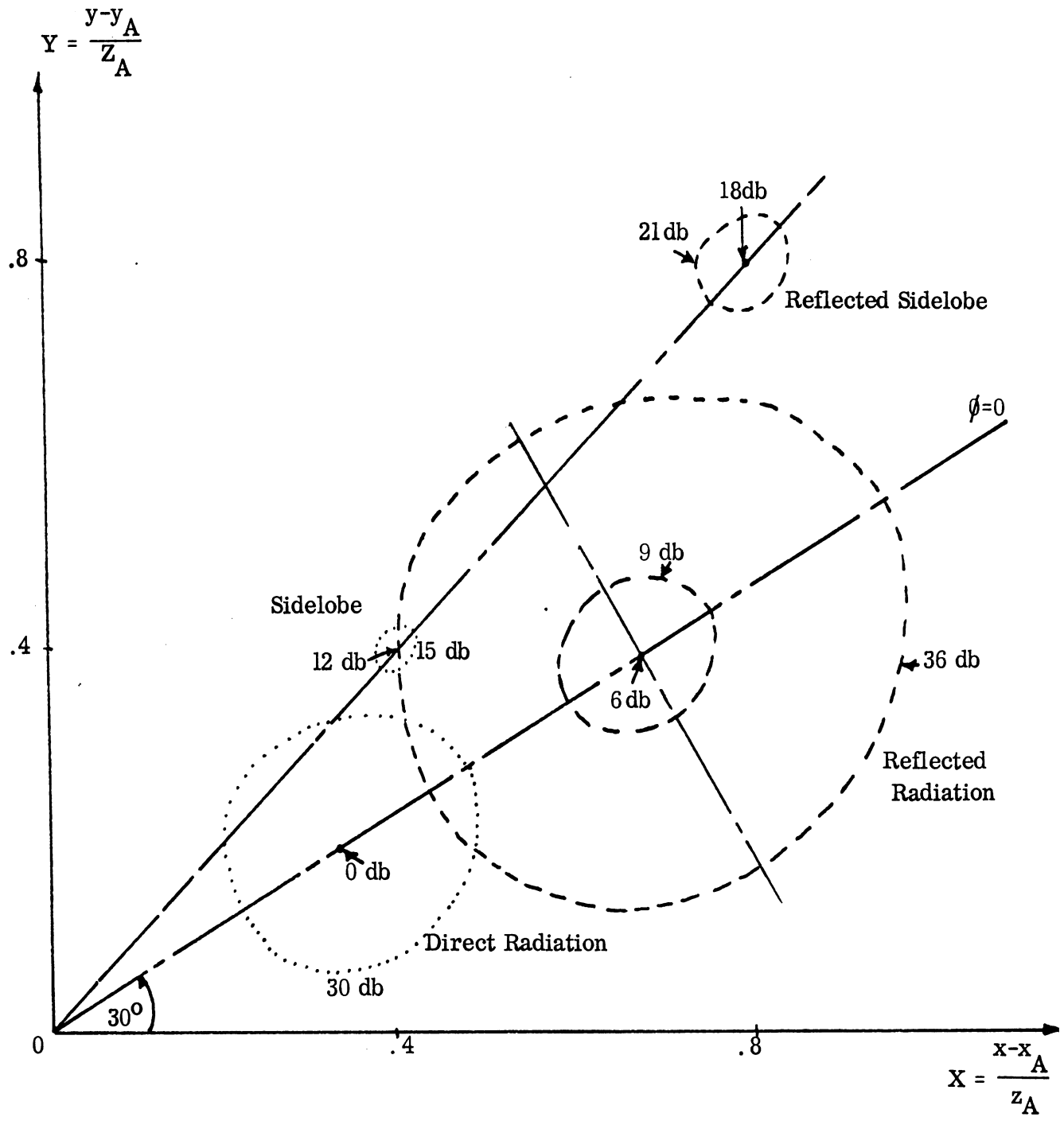

FIG. 13: SPATIAL VARIATION OF ELECTRIC FIELD STRENGTH. Radiation Pattern with main lobe at $\theta_A = 120^o, \phi_A = 30^o$ and sidelobe down 15 db on main lobe and at $\theta_A = 130^o$, $\phi_A = 45^o$, $\xi = 1/2$.

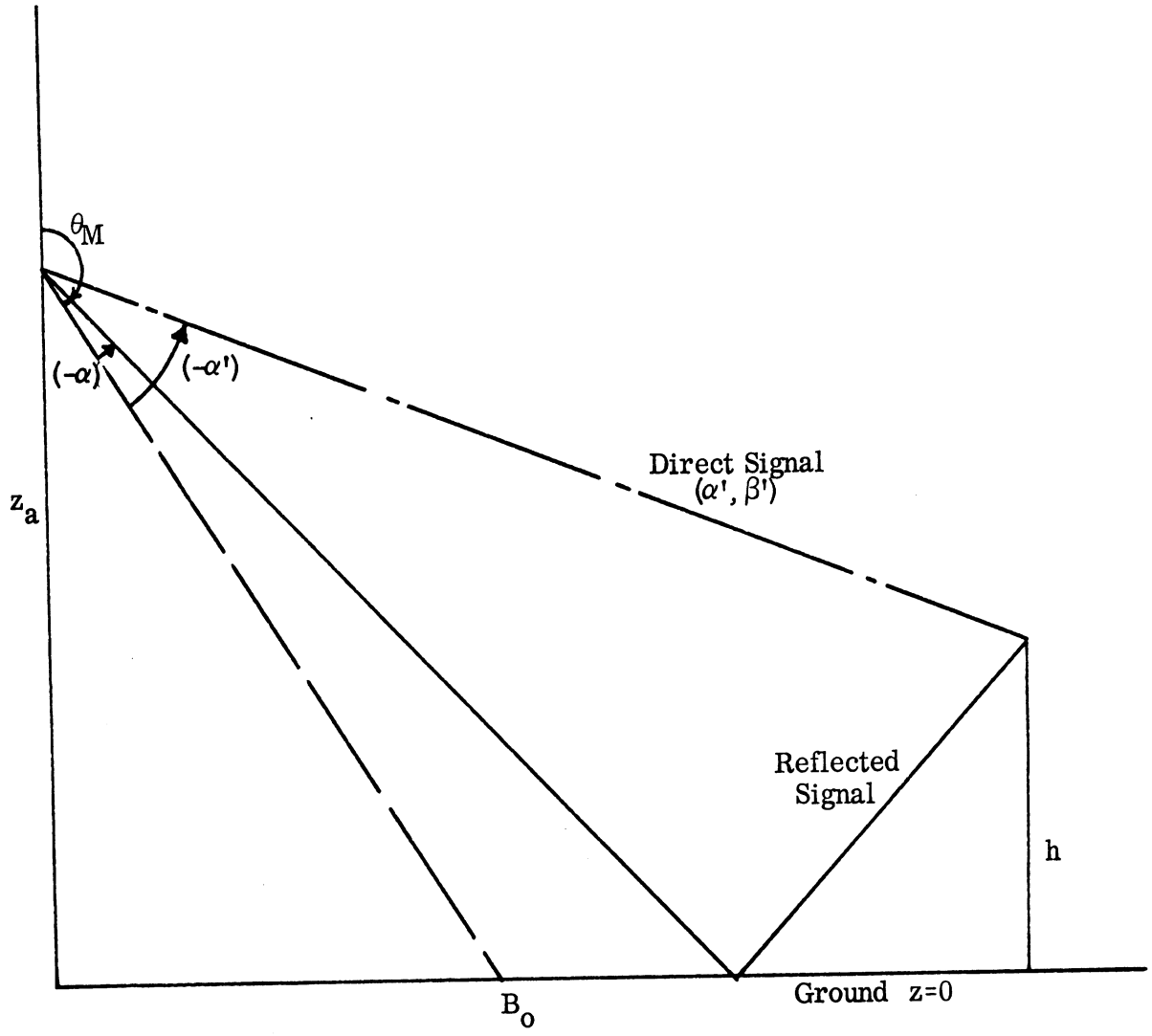

FIG. 14: GEOMETRY FOR DIRECT ARRAY

It is of interest to know when an observer at (X, Y, Z) is measuring predominantly direct signal power rather than indirect or reflected signal power.

Let α', β' define the direction of the direct ray and α, β that of the reflected ray. From the geometry, it is found that

$$\tan(\theta_M+\alpha) = \xi \tan(\theta_M+\alpha')$$

and

$$\tan\beta = \xi \tan\beta' \quad .$$

The locus of points at which $E_h^{(r)}(X, Y)$ equals $E_h^{(d)}(X, Y)$ is given by

$$\frac{1+\tan^2(\theta_M+\alpha)+\sec^2\theta_M\tan^2\beta}{\xi^2+\tan^2(\theta_M+\alpha)+\sec^2\theta_M\tan^2\beta} = \exp\left[a^2(\alpha'^2-\alpha^2)+b^2(\beta'^2-\beta^2)\right] \qquad (A.8)$$

It is noted that this equation may be solved by hand.

To complete this description of the spatial variation of the electric field strength, the sidelobes must be included. As noted above this may be effected by using second-order Bessel functions in the beam pattern function. In this case, it is found that

$$\left|\frac{E_h^{(d)}(X, Y)}{E_h^{(d)}\left(X(\alpha=\beta=0), Y(\alpha=\beta=0)\right)}\right| = \frac{\sec\theta_M}{\left\{\sec^2(\theta_M+\alpha)+\sec^2\theta_M\tan^2\beta\right\}^{1/2}} * 64\frac{J_2(a\alpha')}{(a\alpha')^2}\frac{J_2(b\beta')}{(b\beta')^2}$$

$$\left|\frac{E_h^{(r)}(X, Y)}{E_h^{(r)}\left(X(\alpha=\beta=0), Y(\alpha=\beta=0)\right)}\right| = \frac{\sec\theta_M}{\left\{\sec^2(\theta_M+\alpha)+\sec^2\theta_M\tan^2\beta\right\}^{1/2}} * 64\frac{J_2(a\alpha)}{(a\alpha)^2}\frac{J_2(b\beta)}{(b\beta)^2}$$

and

$$\left| \frac{E_h^{(r)}\left(X(\alpha=\beta=0), Y(\alpha=\beta=0)\right)}{E_h^{(d)}\left(X(\alpha=\beta=0), Y(\alpha=\beta=0)\right)} \right| = \xi \ .$$

Sidelobes are certainly introduced in the above equations. However it is not possible to specify arbitrarily the position of the center of the sidelobe pattern nor the number of db down of the sidelobe on the main lobe. In order to circumvent this problem we compound the pattern from a collection of Gaussian beams, i.e. we use the principle of superimposition[+] Figure 13 shows sidelobes determined in this fashion.

[+]There is a further advantage in specifying the sidelobes in terms of Gaussian Beams. If we wish to find the locus of points for which the reflected radiation equals the direct radiation we have to solve the following equation for θ and ϕ:

$$\xi = \left[\left(\frac{\alpha'}{\alpha}\right)^2 \left(\frac{\beta'}{\beta}\right)^2 \frac{J_2(a\alpha)}{J_2(a\alpha')} \frac{J_2(b\beta)}{J_2(b\beta')} \right] .$$

Clearly, Eq. (A. 7) is more accessible to hand computation.

APPENDIX B

TEMPORAL VARIATIONS IN FIELD STRENGTH FOR A GAUSSIAN BEAM

In Section 3.2, expressions describing the temporal variations of electric field strength were developed. Here, these equations are particularized to the case of a Gaussian beam and CW transmitted signal.

Figure 15 shows an aircraft travelling with X-directed velocity. The fixed observation point is described either by reference to the initial position of the aircraft or to the position of the aircraft at time, t. If $\alpha(t)$ and $\beta(t)$ specify the ray direction from the airplane to the image of the observation point at time t, the following relationships are obtained:

$$\tan\left(\theta_M+\alpha(t)\right)=\tan\left(\theta_M+\alpha(0)\right)+S(t)\cos\phi_A$$

$$\tan\beta(t)=\tan\beta(0)+S(t)\sin\phi_A\cos\theta_m$$

$$\left[R(t)\right]^2=(z_A+h)^2\left\{S^2(t)+S(t)\left[\tan\left(\theta_M+\alpha(0)\right)\cos\phi_A+\sec\theta_M\sin\phi_A\tan\beta(0)\right]+\sec^2\left(\theta_M+\alpha(0)\right)+\sec^2\theta_M\tan^2\beta(0)\right\}$$

and

$$\left[R(0)\right]^2=(z_A+h)^2\left\{\sec^2\left(\theta_M+\alpha(0)\right)+\sec^2\theta_M\tan^2\beta(0)\right\}$$

where

$$S\triangleq\frac{Vt}{(z_A+h)}$$

The ratio of the power level corresponding to a ray at any direction (α, β) at time t to that corresponding to a ray in the direction of maximum power, t=0, at a fixed distance is

$$f^2(\alpha,\beta)\,\frac{R^2(0)}{R^2(t)}\ ,$$

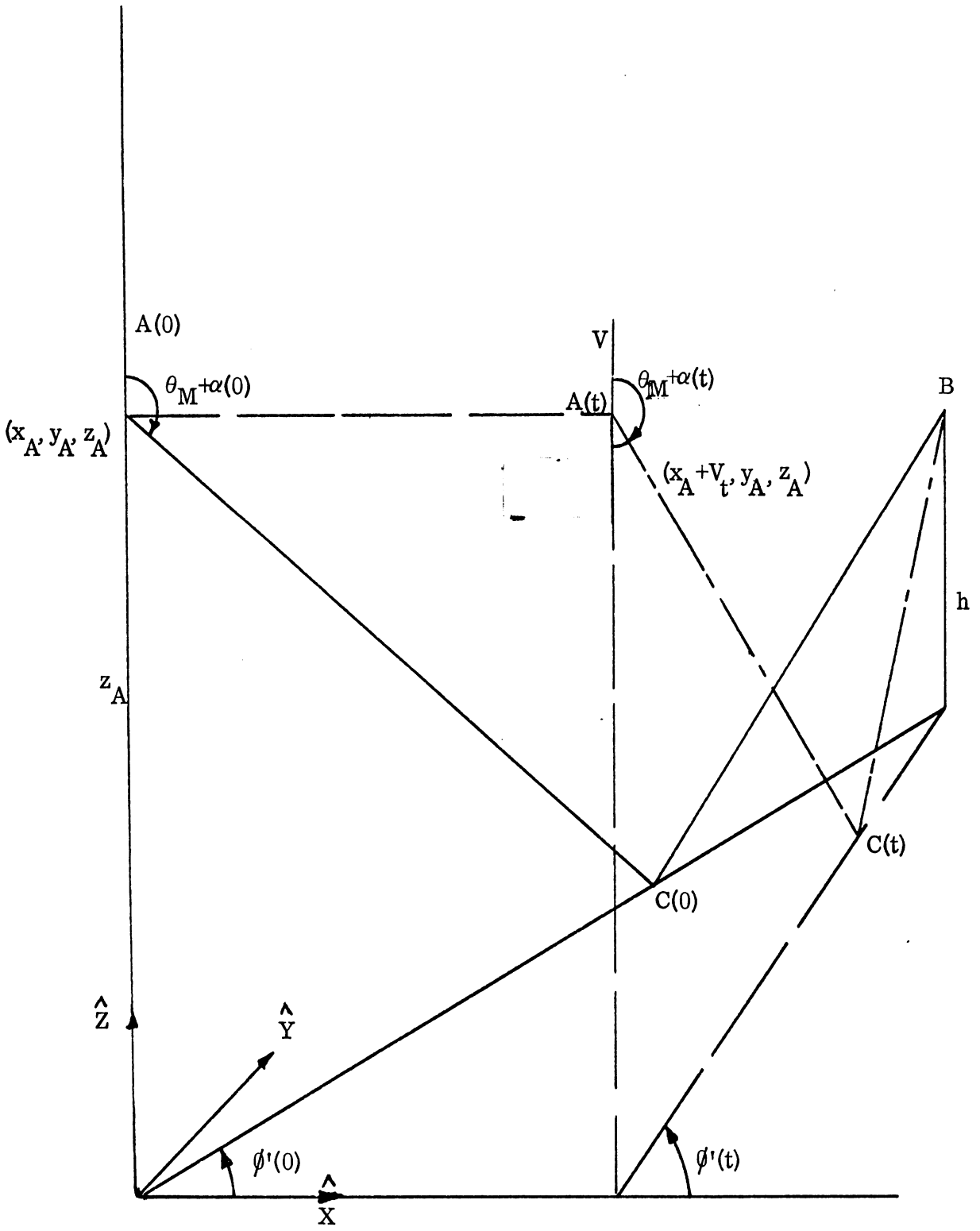

FIG. 15: GEOMETRY FOR AIRPLANE WITH X-DIRECTED VELOCITY, V.

for CW transmitted signal. Denoting this ratio by $F^2(t)$ and recalling the expression for the transmitted Guassian pattern function, we have

$$F^2(t) = \frac{\sec^2(\theta_M+\alpha(0))+\sec^2\theta_M\tan^2\beta(0)\ \exp\left\{-a^2\alpha^2(t)-b^2\beta^2(t)\right\}}{S^2(t)+S(t)\left[\tan(\theta_M+\alpha(0))\cos\phi_A+\sec\theta_M\sin\phi_A\tan\beta(0)\right]+\sec^2(\theta_M+\alpha(0))+\sec^2\theta_M\tan^2\beta(0)} \qquad \text{(B. 1)}$$

Assuming that S(t) is small for some small values of t, the exponential term dominates the expression for F(t) and (B. 1) reduces to

$$F(t) \simeq \exp\left\{-a^2\alpha^2(t)-b^2\beta^2(t)\right\} . \qquad \text{(B. 2)}$$

Also $\alpha(t) \simeq S(t)\cos^2\theta_M\cos\phi_A$

and $\beta(t) \simeq S(t)\cos\theta_M\ \phi_A$.

From Eq. (B. 2) we find that the power level at a fixed point (X', Y', Z') at time t is

$$8.7\left[a^2\cos^2\theta_M\cos^2\phi_A+b^2\sin^2\phi_A\right]\cos^2\theta_M S^2(t) \qquad \text{(B. 3)}$$

db below the power level at t = 0.

If (X', Y', Z') is chosen such that at t= 0, $\alpha(0)=\beta(0)=0$ we find from (B. 1) that the power level at time t is

$$8.7\left[a^2\cos^2\theta_M+b^2\sin^2\phi_A\right]\cos^2\theta_M S^2(t)+10\log R^2(0)-10\log R^2(t) \qquad \text{(B. 4)}$$

db below the power level at t = 0.

Figure 16 shows plots of the expressions (B. 3) and (B. 4) against S(t). It is noted that the term $10\log R^2(0)-10\log R^2(t)$ is very small because the plot of the expression for the power in (B. 3) is almost identical to that for (B. 4). That is to

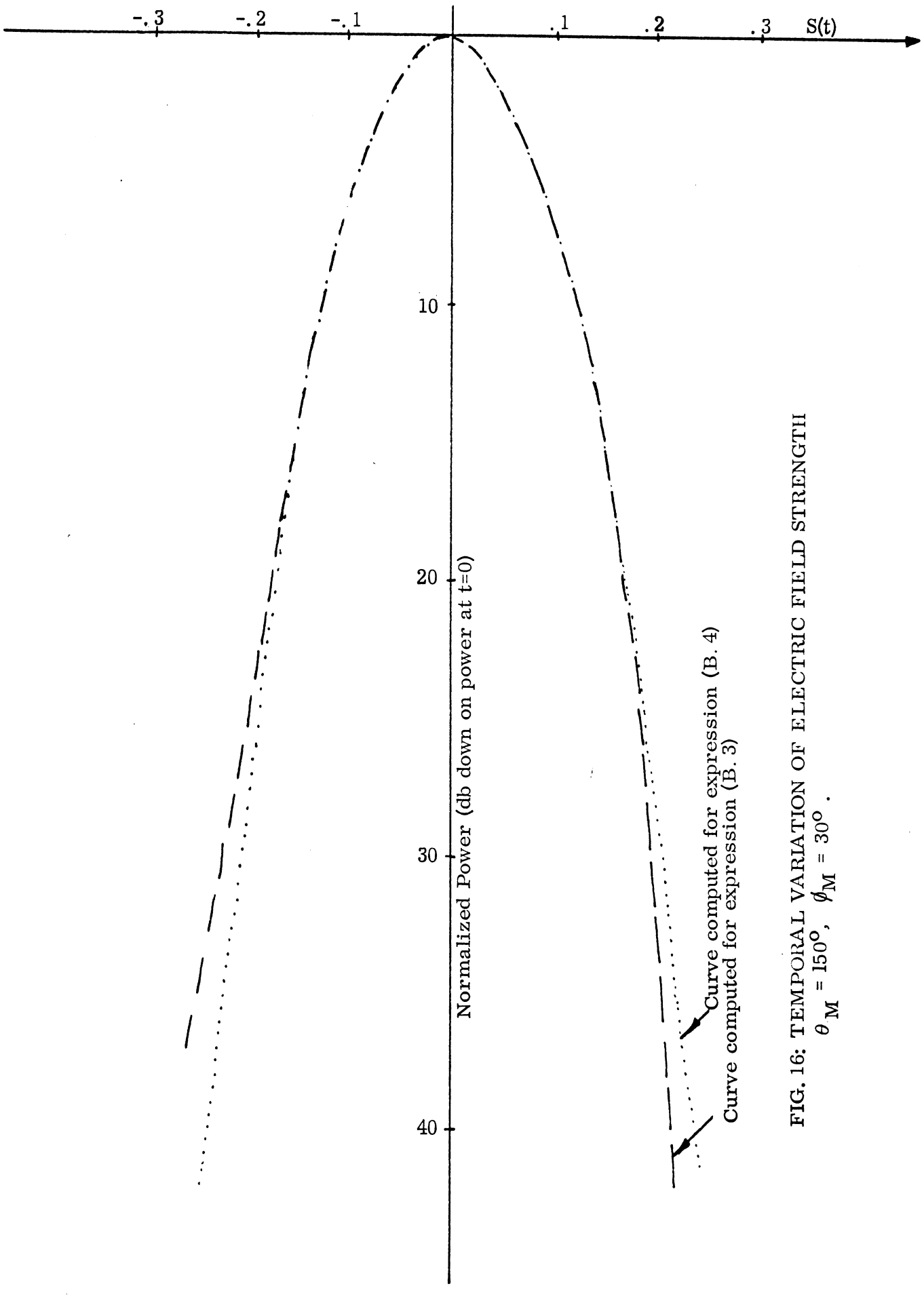

FIG. 16: TEMPORAL VARIATION OF ELECTRIC FIELD STRENGTH
$\theta_M = 150^o$, $\phi_M = 30^o$.

say, for the case chosen, the approximation made above holds.

From Fig. 15 the time an aircraft is 'visible' to an observer, can be approximately computed. For example, if the signal can be detected at 30 db below the maximum received signal and $\theta_M = 150^o$ and $\phi_M = 30^o$, it is found that the normalized time 'visible' is $S_o = 0.44$ and the actual time is given by

$$t = \frac{(z_A + h)S_o}{V} \quad . \tag{B.5}$$

Thus, for an aircraft travelling at 200 knots, an observer at 10,000 ft and an aircraft 70,000 ft, the time 'visible' will be 10.9 secs. Equation (B.5) predicts the expected conclusions that the time 'visible' decreases with lower airplane altitudes and with higher airplane velocities.

UNCLASSIFIED

Security Classification

DOCUMENT CONTROL DATA - R & D

(Security classification of title, body of abstract and indexing annotation must be entered when the overall report is classified)

1. ORIGINATING ACTIVITY *(Corporate author)* The University of Michigan Radiation Laboratory, Dept. of Electrical Engineering, 201 Catherine Street, Ann Arbor, Michigan 48108	2a. REPORT SECURITY CLASSIFICATION UNCLASSIFIED 2b. GROUP

3. REPORT TITLE

DOPPLER RADIATION STUDY

4. DESCRIPTIVE NOTES *(Type of report and inclusive dates)*

Quarterly Report No. 2 1 October 1967 - 1 January 1968

5. AUTHOR(S) *(First name, middle initial, last name)*

Chiao-Min Chu, Joseph E. Ferris and Andrew M. Lugg

6. REPORT DATE	7a. TOTAL NO. OF PAGES	7b. NO. OF REFS
15 January 1968	37	-

8a. CONTRACT OR GRANT NO.	9a. ORIGINATOR'S REPORT NUMBER(S)
N62269-67-C-0545	1082-2-Q
b. PROJECT NO.	
c.	9b. OTHER REPORT NO(S) *(Any other numbers that may be assigned this report)*
d.	-

10. DISTRIBUTION STATEMENT

Requests for this document should be directed to NADC, Johnsville, Warminster, PA 18974

11. SUPPLEMENTARY NOTES	12. SPONSORING MILITARY ACTIVITY
	U. S. Naval Air Development Center Johnsville, Warminster, PA 18974

13. ABSTRACT

In this, the Second Quarterly Report on "Doppler Radiation Study", some results of experimental and theoretical investigation are reported.

The measured antenna pattern data for an AN/APN-153 system obtained during the last quarter has been put into digital, three-dimensional format. This digital data will be used in the theoretical calculation of the direct and reflected radiation. In the theoretical study, a numerical scheme for calculating the spatial and temporal variations of the reflected radiation, based on a perfectly reflecting ground, is formulated. Schemes for presenting the numerical results in terms of 'normalized coordinates' are also considered. For the minimum detectable signal and gain of the possible receiving system, the approximate signal ranges are calculated.

DD FORM 1 NOV 65 1473

UNCLASSIFIED

Security Classification

14. KEY WORDS	LINK A		LINK B		LINK C	
	ROLE	WT	ROLE	WT	ROLE	WT
Doppler Navigational Systems						
Airborne Radar						
Radiation Patterns						
Geometrical Optics						